JOURNAL OF GUIDANCE, CONTROL, AND DYNAMICS
Vol. 26, No. 2, March–April 2003

Frozen Orbits About the Moon

Antonio Elipe*
Universidad de Zaragoza, 50009 Zaragoza, Spain
and
Martín Lara†
Real Instituto y Observatorio de la Armada, 11110 San Fernando, Spain

Frozen orbits are of special interest to mission designers of artificial satellites. On average the eccentricity and argument of the perigee of such orbits remain stationary. Frozen orbits correspond to equilibria in an averaged form of the zonal problem and are almost periodic solutions of the full (nonaveraged) problem. In the zonal problem of a satellite around the moon, we numerically continue natural families of periodic orbits with the polar component of the angular momentum as the parameter. Three families of frozen orbits are discovered.

I. Introduction

AN orbit with almost constant eccentricity and with an almost constant periapse direction (on average) is called a frozen orbit. A low but constant eccentricity ensures a constant altitude, and, for this reason, frozen orbits are recommended for reconnaissance. A fixed argument of the perigee ensures longer living satellites. For Earth, frozen orbits have been studied extensively in the past; a long list of references is given in Ref. 1.

In the case of the moon and problems in connection with natural satellites or asteroids, interest in frozen orbits has developed only recently.[2–5] Park and Junkins[2] obtained frozen orbits for the moon by setting to zero the time derivatives of the instantaneous eccentricity, inclination, and argument of the perigee in the zonal problem of artificial satellite theory. These roots do not correspond to an equilibrium of the problem. Nonetheless, assuming that the root in eccentricity is small and limiting themselves to arguments of perigee equivalent to $\pi/2$ modulo π, these authors adjusted the other Keplerian elements to determine initial conditions for frozen orbits. Eventually, by numerical integration, they ascertained that one of their candidates for initial conditions does indeed produce a frozen orbit of very low eccentricity but very high inclination. Clearly this does not constitute a systematic method for finding families of frozen orbits irrespective of their eccentricity.

We take a different approach. Our tool is a software package designed to continue one-parameter families of periodic orbits for general dynamic systems with two degrees of freedom, yet admitting one integral.[6] The program has two components. With the first one, the corrector, we can solve the following problem: Given initial conditions that produce an almost periodic orbit, how are the initial conditions refined to obtain a tighter closure? With the second component, the predictor, when given a periodic orbit corresponding to a certain value of the parameter, we displace slightly the value and calculate approximately initial conditions for a periodic orbit; then we use the corrector to converge to a periodic orbit. The process is repeated until the family reaches a singularity. Corrector and predictor involve a numerical integration of the differential equations of the system jointly with the variational equations. The variations are essential either to correct or to predict initial conditions. Also note that, from the variations at the end of a period, we extract the characteristic exponents of the orbit; these constitute a measure of the stability of the orbit. The numerical integration we adopt is recognized to be stable. It amounts to decomposing the solution and its variations into a recurrent chain of power series. The program has been applied with success[7] to recover the families of frozen orbits about the Earth that have been conjectured from asymptotic analytical expansions.[1]

Following this procedure we have found three families of frozen orbits around the moon:

1) The S_0 family starts at the equator with orbits of low eccentricities and purely imaginary characteristic exponents. It continues up to an inclination of 90 deg, but with progressively larger eccentricities, and the characteristic exponents at one point change from stability to instability. The family presents two dips in eccentricity at inclinations around 27 and 53 deg, respectively. The first dip seems to be caused by the coefficient $C_{7,0}$, although we have no analytical confirmation of that.

2) The S_1 family starts with an inclination $I = 86.46$ deg, an eccentricity $e = 0.153$, and characteristic exponents both equal to $+1$ and ends with an inclination $I = 73.89$ deg, an eccentricity $e = 0.146$, and characteristic exponents both equal to $+1$. It presents a dip at $I = 78.26$ deg, where the eccentricity reaches the minimum value $e = 0.0002$. The frozen orbit calculated by Park and Junkins[2] belongs to S_1; it is found, as expected, close to the dip in eccentricity.

3) The S_2 family bifurcates from S_1; it is made of unstable orbits with higher than $e = 0.146$ eccentricities. For these reasons, we did not continue it to its termination.

We worked with different models of the gravity potential: Initially we used Akim's model[8]; next we repeated the calculations with Bruce and Ferrari's model.[9] Qualitatively speaking, we did not detect meaningful differences from one model to the other. Later, we received the lunar gravity model (LGM) potential LGM0281 (Ref. 10) from Junkins. Here again, provided we do not take more than 16 coefficients, the behavior of the families does not differ by much. However, this is no longer true if we include harmonics of degree 17–20 in the model. There seems to be a general shift to the right of the dips in eccentricity in the diagrams showing the average eccentricity of a frozen orbit plotted against its average inclination. We did not examine in detail these modifications. The coefficients in the gravity model are not known with complete accuracy; until they are, it serves no purpose to comment on how variations in values affect the existence and behavior of families of periodic frozen orbits. Thus, our conclusions should be limited to claiming that there are many frozen orbits about the moon at any inclination.

The paper is organized as follows. In Sec. II, we recall basic concepts about general dynamic systems with two degrees of freedom and their variational equations both in the Cartesian frame and in the Frenet frame attached to an orbit. In the following section, these concepts are then applied to a mass point about the moon. It is assumed that the density of the moon admits axial symmetry and also that the satellite is sufficiently close to the surface of the moon that perturbation by Earth can be ignored. (Third-body effect of Earth becomes important when the apoapse is greater than about

Received 12 July 2001; revision received 9 January 2002; accepted for publication 14 October 2002.

*Professor, Grupo de Mecánica Espacial. Senior Member AIAA.
†Service Chief, Ephemeris Section.

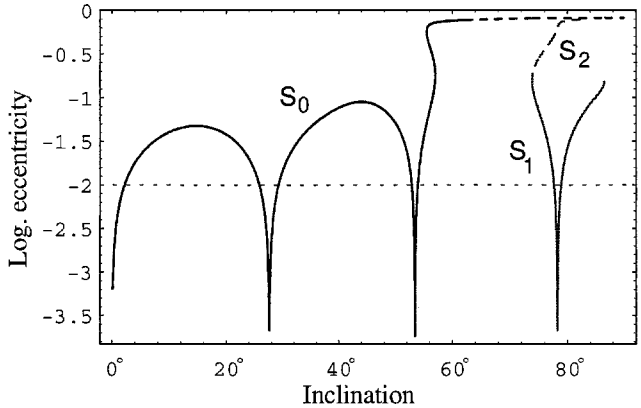

Fig. 1 Families of periodic frozen orbits for the moon; family S_1 are stable orbits, S_2 are unstable ones with high eccentricities, and frozen orbits S_0 are stable for inclination $I \in [0, 63°)$ and unstable for $I \in [63, 90°)$: ——, stable periodic orbits and – – –, unstable orbits.

500 km.) Once the major assumptions making the zonal problem of lunar satellite theory have been set, we show how to continue a family of periodic orbits. The results attained in this paper are shown in Fig. 1.

II. Variational Equations

We shall deal with a problem of two degrees of freedom, for which the equations are written in the form

$$\ddot{x} = 2A(x, y; \sigma)\dot{y} + W_x(x, y; \sigma)$$

$$\ddot{y} = -2A(x, y; \sigma)\dot{x} + W_y(x, y; \sigma) \tag{1}$$

with A and W functions of the coordinates x and y and of a parameter σ that will be specified later. Obviously, these equations have the energy integral

$$C = 2W - (\dot{x}^2 + \dot{y}^2) \tag{2}$$

that is sometimes referred to as the Painlevé constant.

Any solution

$$x(t; \sigma), \qquad y(t; \sigma) \tag{3}$$

of Eq. (1) depends on σ. The displacements

$$\delta x = \frac{\partial x}{\partial \sigma}\delta\sigma, \qquad \delta y = \frac{\partial y}{\partial \sigma}\delta\sigma, \qquad \delta\dot{x} = \frac{\partial \dot{x}}{\partial \sigma}\delta\sigma, \qquad \delta\dot{y} = \frac{\partial \dot{y}}{\partial \sigma}\delta\sigma$$

of Eq. (3) induced by a variation of the parameter σ will be solution of the variational equations

$$\delta\ddot{x} = 2A\delta\dot{y} + (W_{xx} + 2A_x\dot{y})\delta x + (W_{xy} + 2A_y\dot{y})\delta y + (W_{x\sigma} + 2A_\sigma\dot{y})\delta\sigma$$

$$\delta\ddot{y} = -2A\delta\dot{x} + (W_{xy} - 2A_x\dot{x})\delta x + (W_{yy} - 2A_y\dot{x})\delta y + (W_{y\sigma} - 2A_\sigma\dot{x})\delta\sigma \tag{4}$$

and they satisfy the variational integral

$$\mathcal{J} = W_\sigma\delta\sigma + W_x\delta x + W_y\delta y - \dot{x}\delta\dot{x} - \dot{y}\delta\dot{y} \tag{5}$$

We will look for isoenergetic variations, that is, those for which $\mathcal{J} = 0$. Let us assume that for a given value of the parameter σ we find a periodic solution of Eq. (1). With Eqs. (4) and (5), we obtain an approximate periodic solution for a value of the parameter $\sigma + \delta\sigma$. The main difficulty that we encounter is that the secular and periodic solutions are mixed, which may degenerate the solution. To avoid this, Deprit and Henrard[6] invented an algorithm that converts the variational equations (4) into an equivalent system for the normal n and tangential p displacements. In this way, the secular displacements (the tangential) are split from the purely periodic ones (the normal).

The variations of the Cartesian coordinates are related with the intrinsic displacements through the relations

$$\delta x = p\cos\phi - n\sin\phi, \qquad \delta y = p\sin\phi + n\cos\phi$$

$$\delta\dot{x} = \dot{p}\cos\phi - \dot{n}\sin\phi - \dot{\phi}\delta y, \qquad \delta\dot{y} = \dot{p}\sin\phi + \dot{n}\cos\phi + \dot{\phi}\delta x \tag{6}$$

where the angle ϕ is the inclination of the velocity vector over the x-axis. Deprit and Henrard[6] proved that the normal isoenergetic displacement n satisfies the equation

$$\ddot{n} + \Theta n = -2W_\sigma[(A + \dot{\phi})/V] - 2A_\sigma V + W_{y\sigma}\cos\phi - W_{x\sigma}\sin\phi \tag{7}$$

the coefficient Θ in the left-hand member is

$$\Theta = \ddot{V}/V + 2(A + \dot{\phi})^2 + 2A^2 - W_{xx} - W_{yy} - 2V(A_x\sin\phi - A_y\cos\phi)$$

Once Eq. (7) is solved, the tangential displacement results from the quadrature

$$\frac{\mathrm{d}}{\mathrm{d}t}\left(\frac{p}{V}\right) = 2\frac{A + \dot{\phi}}{V}n + \frac{W_\sigma}{V^2} \tag{8}$$

The general solution of Eq. (7) is the linear combination

$$n = \alpha n^{\mathrm{I}} + \beta n^{\mathrm{II}} + n^\sigma$$

where n^{I} and n^{II} are solutions of the homogeneous part of Eq. (7) for the set of initial conditions

$$n^{\mathrm{I}}(0) = \dot{n}^{\mathrm{II}}(0) = 1, \qquad \dot{n}^{\mathrm{I}}(0) = n^{\mathrm{II}}(0) = 0 \tag{9}$$

and n^σ is a particular solution of Eq. (7) for the initial values

$$n^\sigma(0) = \dot{n}^\sigma(0) = 0 \tag{10}$$

Analogously, the tangential displacement is obtained as the linear combination

$$p = \alpha p^{\mathrm{I}} + \beta p^{\mathrm{II}} + p^\sigma$$

where p^{I} and p^{II} result from quadratures of the form

$$\frac{\mathrm{d}}{\mathrm{d}t}\left(\frac{p}{V}\right) = 2\frac{A + \dot{\phi}}{V}n \tag{11}$$

corresponding, respectively, to n^{I} and n^{II} for the initial condition $p(0) = 0$, whereas p^σ is the particular solution of Eq. (8) for n^σ. The coefficients α and β are determined by the initial conditions $n(0)$ and $\dot{n}(0)$ and the conditions of periodicity. With this, α and β stem from the linear system

$$\alpha[n^{\mathrm{I}}(T) - 1] + \beta n^{\mathrm{II}}(T) = -n^\sigma(T)$$

$$\alpha\dot{n}^{\mathrm{I}}(T) + \beta[\dot{n}^{\mathrm{II}}(T) - 1] = -\dot{n}^\sigma(T) \tag{12}$$

where T is the period of the periodic orbit, provided that the trace of the resolvent for Hill's equation

$$\mathrm{tr}(T) = n^{\mathrm{I}}(T) + \dot{n}^{\mathrm{II}}(T) \tag{13}$$

is not equal to 2. The point at which the trace is 2 marks what Wintner[11] calls the "termination" of the family. The trace thus computed plays a very important role because it gives the stability of the computed orbit. When $|\mathrm{tr}(T)| < 2$, the characteristic exponents of the orbit are of the stable type; if $|\mathrm{tr}(T)| > 2$, they are of unstable type, whereas $|\mathrm{tr}(T)| = 2$ represents cases of indifferent stability.

Once the constants α and β are computed from Eq. (12), then Eqs. (6) together with the initial conditions (9) and (10) will provide the corrections to the periodic orbit.

Deprit and Henrard[6] gave the method for continuing natural families of periodic orbits parametrized by the Painlevé constant.

Lara et al.[7] produced an adaptation of the method for another parameter, provided the potential is of the form

$$W = -\sum_{i>0} \sigma_i F_i(x, y) \tag{14}$$

where σ_i are the parameters of the problem. The variational equations will correspond to one parameter chosen among these σ_i. More recently, Lara[12] extended the method for a more general parametric case.

The method developed in Ref. 7 is valid for any zonal gravity field, although the authors mainly focused on continuing numerically families of periodic orbits to the Earth zonal satellite problem. In the following sections, we apply the same method to the moon zonal satellite problem.

III. Zonal Problem for the Moon Potential

The potential of the moon, when only zonal harmonics are considered, is of the form

$$\mathcal{V} = -\frac{\mu}{r} + \frac{\mu}{r} \sum_{2 \le n \le m} \left(\frac{\alpha}{r}\right)^n J_n P_n(u) \tag{15}$$

where μ is the gravitational constant of the moon, r is the radial distance, u is z/r, α is the equatorial radius of the moon, J_n is the zonal coefficient of degree n, and P_n is the Legendre polynomial of degree n.

There is no agreement regarding the gravity field model for the moon, and the coefficients are different in each model. See Table 1 in which we give two models. In this work, we choose the 7×7 Akim's gravity model[8] as given in Table 1, although we computed periodic orbits for other models and obtained similar results.

As to the Earth's potential, the dominant coefficient is J_2; the rest are of higher order, but in contrast to the Earth, the coefficient J_7 is larger than the previous ones (J_3–J_6), which might have a strong influence on the periodic orbits.

The motion of a particle orbiting the moon is a problem of three degrees of freedom. However, when only the influence of the zonal harmonics is considered, the Hamiltonian is invariant to rotations around the polar axis, and, consequently, the polar component Λ of the angular momentum vector $\boldsymbol{G}$ is an integral of motion, which allows a reduction to two degrees of freedom. Indeed, by the use of cylindrical coordinates ρ, z, λ, P, Z, and Λ, the Hamiltonian takes the form

$$\mathcal{H} = \tfrac{1}{2}(P^2 + Z^2 + \Lambda^2/\rho^2) + \mathcal{V}(\rho, z)$$

and it may be rewritten as

$$\mathcal{H} = \tfrac{1}{2}(P^2 + Z^2) - W(\rho, z) \tag{16}$$

with the effective potential function

$$W = -\Lambda^2/2\rho^2 - \mathcal{V}(\rho, z)$$

The moment Λ being an integral, its conjugate coordinate λ will be obtained (once the problem integrated) by the quadrature

$$\lambda = \Lambda \int_0^t \frac{\mathrm{d}t}{\rho(t)^2}$$

Table 1 Zonal coefficients from the 7×7 Akim's[8] gravity model of the moon and from Goddard Lunar Gravity Model-1 (GLGM-1)

Coefficient	Akim[8]	GLGM-1
J_2	0.2070×10^{-3}	$2.037448533865259 \times 10^{-4}$
J_3	0.4900×10^{-5}	$1.026274048885357 \times 10^{-5}$
J_4	0.8000×10^{-6}	$-9.008534083140000 \times 10^{-6}$
J_5	-0.3600×10^{-5}	$1.243678088670680 \times 10^{-6}$
J_6	-0.1100×10^{-5}	$-1.362456275204084 \times 10^{-5}$
J_7	-0.2870×10^{-4}	$-2.558744417452570 \times 10^{-5}$

In this way we separate the motion of the satellite in its meridian plane from the rotation of that plane. Moreover, the rotation of the meridian plane includes the effect of the precession of the nodes, which will rarely be commensurate with the intrinsic frequency of the satellite in its orbit. Thus, we will pay no attention to the λ coordinate and will deal with orbits that are periodic in the meridian plane and are quasi periodic in three-dimensional space.

The Hamiltonian (16) does not depend explicitly on the independent variable t; thus, the energy of the satellite is preserved along the motion, and we may introduce the energy constant C (for the sake of simplifying the notation in the algorithm) as

$$\mathcal{H}(P, Z, \rho, z; \Lambda) = -\tfrac{1}{2}C$$

The equations of the motion corresponding to the Hamiltonian (16) may be written in the same form as Eq. (1):

$$\ddot{\rho} = W_\rho, \qquad \ddot{z} = W_z \tag{17}$$

The differential variational equations (4) are now

$$\begin{aligned} \delta\ddot{\rho} &= W_{\rho\rho}\delta\rho + W_{\rho z}\delta z + W_{\rho\Lambda}\delta\Lambda \\ \delta\ddot{z} &= W_{z\rho}\delta\rho + W_{zz}\delta z + W_{z\Lambda}\delta\Lambda \end{aligned} \tag{18}$$

The variational integral (5) is

$$W_\rho\delta\rho + W_z\delta z - \dot{\rho}\delta\dot{\rho} - \dot{z}\delta\dot{z} - \tfrac{1}{2}\rho^{-2} = 0 \tag{19}$$

Because we shall integrate both systems (17) and (18) numerically, instead of the family itself, we will compute the continuation of the initial conditions ρ_0, z_0, $\dot{\rho}_0$, and $\dot{z}_0$. Formulas and details of the procedure are given by Deprit and Henrard[6] and by Lara et al.[7]

IV. Integration by Recurrent Power Series

For the numerical integration, we employ the method of recurrent power series,[13] although classical Runge–Kutta methods can also be used or even more refined ones such as the multiple shooting technique.[14] Because we have to integrate a differential system and its variational equations, this method is very convenient because it has both high accuracy and stability.[15,16] The integration code is written in FORTRAN 77 using double precision. Note that the FORTRAN programs have not been produced by hand but by machine through an algebraic processor.[13] The generator program assumes that the right-hand members of the differential system are recurrent trees of elementary functions. The generator program goes down each tree, replacing each node by an algorithm generating the corresponding power series. Proceeding in this way, we overcome the major objection made to the method of integration by recurrent power series, namely, that it is necessary to write a specific program for each differential system. Once it is built and tested, the program generator takes care of adapting the method to any particular system in a rather wide set of differential equations. (See Ref. 13 for details.)

By the simple expedient of adopting new units of length and time, we can make the Gaussian constant $\mu = 1$ and consider only the value $C = 1$ for the energy integral without loss of generality. In the new units, the tolerance for periodicity is 10^{-13}, that is, we say that an orbit is periodic when the difference between one point at the epoch t and the initial point is $\le 10^{-13}$. The same criterion has been applied to check the different control identities along the integration.

The natural families we follow are parametrized by Λ; however, they are made of frozen orbits, and these orbits are characterized by an average eccentricity $\langle e \rangle$ and an average inclination $\langle I \rangle$. These characteristics are computed numerically by calculating the integrals

$$\langle e \rangle = \frac{1}{T}\int_0^T e(t)\,\mathrm{d}t, \qquad \langle I \rangle = \frac{1}{T}\int_0^T I(t)\,\mathrm{d}t$$

To these numbers, we add the stability index (13). We collect these individual characteristics in a plot $\langle I \rangle$ vs $\langle e \rangle$, where the natural family becomes a curve.

By definition, the argument of pericenter g for a frozen orbit is stationary on average, that is, $\mathrm{d}\langle g\rangle/\mathrm{d}t = 0$. The average $\langle g\rangle$ is inaccessible to us because we operate immediately on the original equations of motion. Instead, for each periodic orbit, we compute the values

$$\gamma = \min_{t\in T} g(t) \qquad \Gamma = \max_{t\in T} g(t)$$

The difference $\delta g = |\Gamma - \gamma|$ is a measure of the maximum elongation of the osculating argument of the pericenter from its average value. The smaller δg is, the closer the periodic orbit is to a frozen orbit.

V. Frozen Orbits

To start the S_0 family, we start with a circular equatorial initial conditions $\rho = 1$, and $z = \dot\rho = 0$, with the value of the parameter $\Lambda \approx G$. With these initial conditions, the corrector rapidly converges to a periodic orbit of the J_2–J_7 problem. Thus, by construction, S_0 begins with a quasi-circular equatorial orbit, but soon the eccentricity grows to a maximum. Thereafter it decreases until it reaches a minimum for an inclination $I \approx 27.6$ deg. From there, the eccentricity increases again, but quickly, to a new maximum, then decreases to almost 0 for $I \approx 53.4$ deg and again climbs swiftly to almost 1. This high eccentricity remains almost unchanged while the inclination increases up to $\pi/2$ (Fig. 1). According to the stability index, S_0 is made of stable orbits from the value $I = 0$ deg ($\Lambda = G$) until the inclination reaches a value $I \approx 63$ deg. At this point, the orbits become unstable until the end of the family at $\pi/2$. A period doubling, pitchfork bifurcation occurs at $I \approx 63$ deg.

Starting the S_1 family is a little more complicated than for the S_0 family. We sweep inclinations down starting from the polar case and eventually found starting orbits by adjusting a quasi-circular orbit with large inclination. Once the family was started, we moved the parameter Λ in both directions. This technique produces a family that we labeled S_1. Continuation of S_1 by increasing Λ showed that this family terminates at an inclination close to 73 deg, while the continuation in the opposite direction revealed that orbits in S_1 near the inclination $\pi/2$ have very large eccentricities. Indeed, the minimum value of the eccentricity ($e \approx 10^{-3.4}$) for this family is found at an inclination $I \approx 78.2$ deg. The stability index (13) shows that all orbits of S_1 are stable.

Knowledge of previous results on periodic orbits in the zonal problem for other celestial bodies (Earth and Mars) prompted us to look for yet another natural family of periodic orbits, starting from an inclination and eccentricity near the ones where the family S_1 ends. To obtain initial conditions for an orbit in that family, we took the initial conditions of an orbit in the family S_1 close to the termination, and then we varied slightly these initial conditions with the view of increasing the eccentricity but maintaining the period. After several trials with different initial conditions, the algorithm converged to a periodic orbit of a new family S_2. The continuation of the family S_2 in both directions (increasing and decreasing inclinations) shows that the family is made of highly eccentric orbits that are all unstable. On the side of decreasing inclinations, with the numerical precision used for the numerical integration, it seems that the families S_1 and S_2 have the same termination.

Poincaré sections are used to corroborate all of those features. In that representation, an orbit is mapped onto a collection of points obtained as the intersection of the orbit with a section (when possible) orthogonal to the flux. Periodic orbits appear as fixed points on the surface and closed trajectories on the surface correspond to regular areas of quasi-integrable motion.

Thus, in Fig. 2 we present three sections $(\rho, \dot\rho)$ for $z = 0$ and $\dot z > 0$. In this representation, almost circular orbits cut the section $z = 0$ with $\dot\rho \approx 0$. However, eccentric orbits cut the plane $z = 0$ with $\dot\rho \neq 0$; the longer the eccentricity of the orbit is the greater the value of $\dot\rho$ is.

The sequence starts with Fig. 2a, corresponding to the inclination $I \approx 63$ deg. At this time, we only find one fixed point corresponding to one periodic orbit of the S_0 family. This fixed point is far away from the origin (1, 0), and therefore, the orbit is highly eccentric. The sequence continues with Fig. 2b, which corresponds to $I \approx 73$ deg. A pitchfork bifurcation occurred with the consequent change in the stability of the (highly eccentric) orbits of S_0. Figure 2c presents the final situation, where a saddle-node bifurcation gives birth to both the stable, almost circular orbits of the S_1 family, the elliptic fixed point close to (1, 0), and the unstable, eccentric orbits of the S_2 family, the hyperbolic fixed point of the section.

For orbits belonging to natural families S_0 (Fig. 3a) and S_1 (Fig. 3b), we plot vertical segments of length δg, that is, to each orbit, we associate the maximum variation of the periapse along a period. By doing so, we provide in Fig. 3 the $(e, \delta g)$ characteristic of the frozen orbit together with the inclination of the orbit. Note in Fig. 3 that the periapse of orbits with eccentricity $e > 1/100$ is clearly frozen. For orbits with smaller eccentricities, the oscillation of the periapse is greater than 3 deg, but this is not relevant because the periapse is not defined for circular orbits.

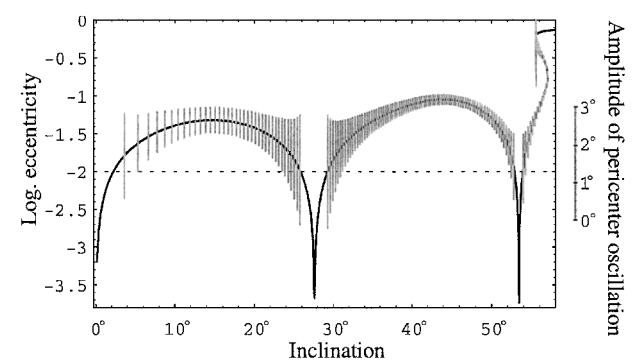

a) S_0

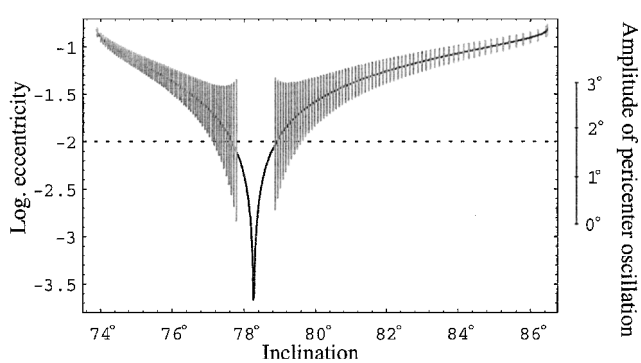

b) S_1

Fig. 3 Variation of the argument of the pericenter, including scale the vertical segments (δg), along the families.

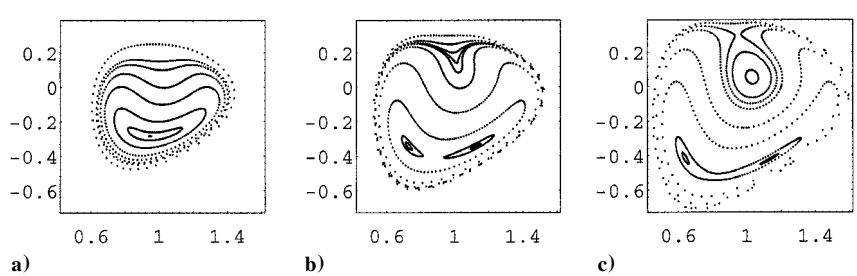

Fig. 2 Poincaré sections with ρ abscissa axis and $\dot\rho$ ordinates axis: a) and b) pitchfork bifurcation of S_0 family and b) and c) saddle-node bifurcations of the S_1 family that gives rise to the S_2 family.

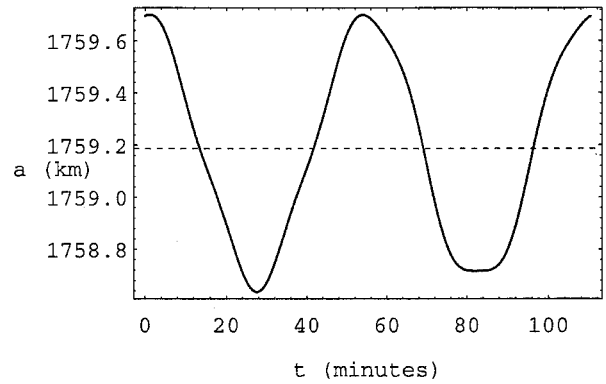

Semimajor axis

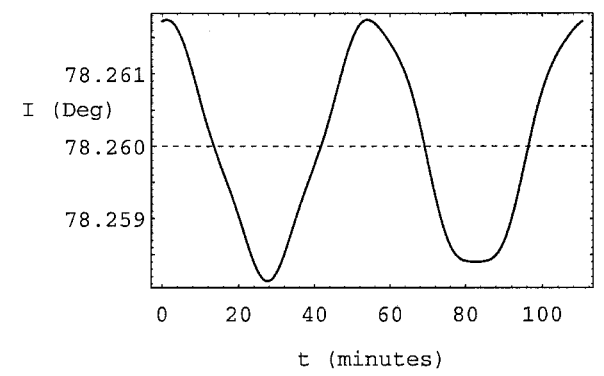

Inclination

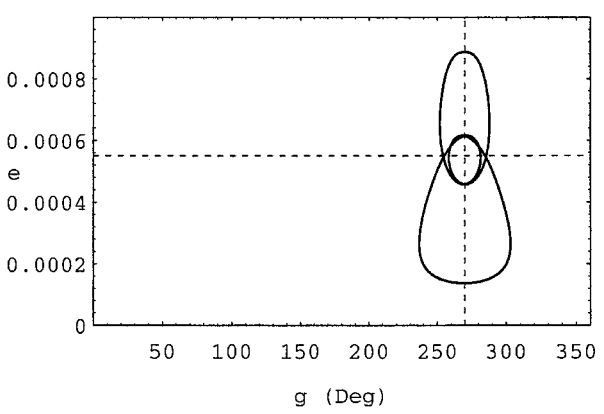

Frozen orbit condition $e = e(g)$

Fig. 4 Typical behavior of a frozen periodic orbit.

To illustrate the behavior of the frozen orbits computed, we take one of them and compute the time evolution over one period of certain orbital elements, namely, the semimajor axis a, the inclination I, and also the frozen orbit condition, that is, eccentricity e vs periapse g. The result is shown in Fig. 4. In our example, we took an orbit with averaged orbital elements $a = 1759.2$ km (some 20 km above the surface of the moon), $e = 0.00055$ (close to the minimum in eccentricity of the S_1 family), $I = 78.26$ deg, and $g = 270$ deg. The nodal period of this orbit is $P \approx 1.84$ h, and these orbital elements are periodic for our zonal model, yet the argument of the node has retrograde secular motion. Albeit this orbit has a very low osculating eccentricity (always less than one thousandth), the osculating periapse remains within the interval $236.75 < g < 303.25$ deg, spending most of the time very close to $g = 270$ deg, the constant averaged value.

The behavior of the periapse is very different even for very close orbits, as we can see in Fig. 5. In Fig. 5, we plot the curve $e = e(g)$ of a frozen orbit with averaged orbital elements $a = 1759.486$ km, $e = 0.0136$, and $I = 78.3$ deg, quite close to the preceding case, but with averaged periapse $g = 90$ deg. Now, the osculating periapse always is $89 < g < 91$ deg (Fig. 5a).

Note that we may have orbital elements slightly different from the ones of a frozen orbit; however, the orbit is not periodic. This is

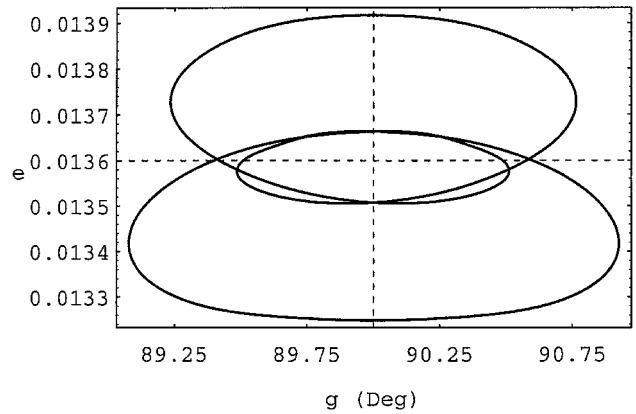

a) Frozen orbit

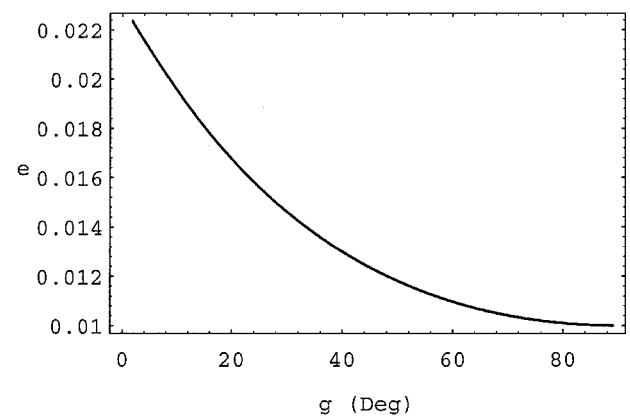

b) Nonfrozen orbit

Fig. 5 Time evolution (3 years) of eccentricity e and periapse g for two orbits with almost equal initial conditions.

shown in Fig. 5b. Indeed, for example, if we take one orbit with initial averaged orbital elements $a = 1759.207$ km, $e = 0.01$, $I = 78.3$ deg, and $g = 89.5$ deg, very close to the preceding case, this orbit is no longer frozen, as we can see in the evolution of eccentricity and periapse that in 3 years goes from 0 to 90 deg.

VI. Conclusions

Frozen orbits that are equilibrium solutions of the averaged problem correspond to quasi-periodic orbits in the original problem. These type of orbits, as with the Earth, are of great interest for lunar orbiters. By continuing natural families of periodic orbits in the zonal problem of the moon, we found three families of periodic orbits that correspond to frozen orbits, that is, that maintain their eccentricity, inclination, and periapse constant along a period. These frozen orbits are very sensitive to the initial conditions, with slightly different orbital elements to the ones we found that do not provide frozen orbits.

Acknowledgments

This work has been supported by the Spanish Ministry of Science and Technology (Project ESP2002-023929) and by the Département de Mathématiques Spatiales at the Centre National d'Études Spatiales (Toulouse, France). We are deeply grateful to A. Deprit, who motivated this work. We acknowledge also his suggestion to present frozen orbits as given in Fig. 3, inspired by the famous C. J. Minard's map (1861) of the Napoleon's March to Russia 1812. Thanks are due to J. L. Junkins for providing us with the LGM0281 gravity model.

References

[1] Coffey, S., Deprit, A., and Deprit, E., "Frozen Orbits for Satellites Close to an Earth-Like Planet," *Celestial Mechanics and Dynamical Astronomy*, Vol. 59, No. 1, 1994, pp. 37–72.

[2] Park, S. Y., and Junkins, J. L., "Orbital Mission Analysis for a Lunar Mapping Satellite," *Journal of the Astronautical Sciences*, Vol. 43, No. 2, 1995, pp. 207–217.

[3]Scheeres, D. J., Guman, M. D., and Villac, B. F., "Stability Analysis of Planetary Satellite Orbiters: Application to the Europa Orbiter," *Journal of Guidance, Control, and Dynamics*, Vol. 24, No. 4, 2001, pp. 778–787.

[4]Scheeres, D. J., Williams, B. G., and Miller, J. K. F., "Evaluation of the Dynamics Environment of an Asteroid: Application to 433 Eros," *Journal of Guidance, Control, and Dynamics*, Vol. 23, No. 3, 2000, pp. 466–475.

[5]Lara, M., and Sheeres, D. J., "Stability Bounds for Three Dimensional Motion Close to Asteroids," American Astronautical Society, Paper AAS 02-108, Jan. 2002.

[6]Deprit, A., and Henrard, J., "Natural Families of Periodic Orbits," *Astronomical Journal*, Vol. 72, No. 2, 1967, pp. 158–172.

[7]Lara, M., Deprit, A., and Elipe, A., "Numerical Continuation of Frozen Orbits for the Zonal Problem," *Celestial Mechanics and Dynamical Astronomy*, Vol. 62, No. 2, 1994, pp. 167–181.

[8]Akim, E.,"Determination of the Gravity Field of the Moon from Movement of Artificial Satellite of the Moon 'Luna-10,' " *Doklady Akademii Nauk USSR*, Vol. 170, 1966, pp. 799–802.

[9]Bruce, G. B., and Ferrari, A. J., "A Harmonic Analysis of Lunar Gravity," *Journal of Geophysical Research*, Vol. 85, No. B2, 1980, pp. 1013–1025.

[10]Lemoine, F. G., Smith, D. E., and Zuber, M. T., "Goddard Lunar Gravity Model-1 (GLGM-1) A 70th Degree and Order Gravity Model for the Moon," *EOS, Transactions, American Geophysical Union*, Vol. 75, No. 41, 1994, p. 400.

[11]Wintner, A., *Analytical Foundations of Celestial Mechanics*, Academic Press, New York, 1931.

[12]Lara, M., "On Numerical Continuation of Families of Periodic Orbits in a Parametric Potential," *Mechanics Research Communication*, Vol. 23, No. 3, 1996, pp. 291–298.

[13]Lara, M., Elipe, A., and Palacios, M., "Automatic Programming of Recurrent Power Series," *Mathematics and Computers in Simulation*, Vol. 49, Nos. 4–5, 1999, pp. 349–360.

[14]Rández, L., "Improving the Efficiency of the Multiple Shooting Technique," *Computers in Mathematics and Applications*, Vol. 24, No. 7, 1992, pp. 127–132.

[15]Deprit, A., and Price, J., "The Computation of Characteristic Exponents in the Planar Restricted Problem of Three Bodies," *Astronomical Journal*, Vol. 70, No. 10, 1965, pp. 836–846.

[16]Deprit, A., and Zahar, R. V. M., "Numerical Integration of an Orbit and Its Concomitant Variations by Recurrent Power Series," *Zeitschrift für Angewandte Mathematik und Physik*, Vol. 17, No. 3, 1966, pp. 425–430.